Optimization of a Grid-Connected Hybrid Energy System with Battery Storage for Hydrogen Production in South Africa

Esmeralda Mukoni and Karen S. Garner, *Senior Member, IEEE*

***Abstract*—This paper presents an optimization study for a grid-connected hybrid energy system combining wind, solar PV, and a battery energy storage system (BESS) for hydrogen production. To address the intermittency of wind and solar resources, the grid compensates for insufficient energy to meet the electrolyzer load demand, while excess or curtailed energy is stored in the BESS to enhance reliability. The study employs a constrained multi-objective non-dominated genetic algorithm within the Python-based Pymoo framework. The optimization identifies an ideal grid-connected hybrid energy system with minimized electricity costs and maximized efficiency at high reliability. Subsequently, the BESS is optimized to reduce storage and electricity costs while maintaining reliability. The optimized BESS is successfully integrated into the hybrid system. Cost of electricity and reliability are assessed based on time-of-use tariffs and loss of power supply probability, respectively. Using a 2 MW proton exchange membrane electrolyzer, the study achieves a highly efficient hybrid system with the BESS applied to six Renewable Energy Development Zones in South Africa. Including the BESS reduces electricity costs, improves reliability, and lowers curtailment ratios by 40-66%.**

***Index Terms*—Battery Energy Storage System, Cost of Electricity and Storage, Non-dominated Sorting Algorithm, Pymoo, Reliability, Renewable Energy**

I. Introduction

Climate change and energy security remain critical global challenges due to the continued reliance on depleting fossil fuels that emit greenhouse gases [2]. To address these issues, renewable energy (RE) has been adopted as a pathway toward decarbonization and alignment with the 2015 Paris Climate Agreement [2]. Among RE technologies, wind and solar PV are the most widely utilized, given their maturity and widespread availability [3]. Alongside RE, there has been increasing adoption of green hydrogen, a clean energy carrier with versatile applications that accelerate decarbonization and enhance energy security [4]. Green hydrogen is produced using RE for water electrolysis, typically employing technologies such as alkaline and Proton Exchange Membrane (PEM) electrolyzers [5]. However, the intermittent nature of RE sources poses challenges in consistently meeting the electrolyzer's load demand. To overcome this, RE sources can be hybridized, enhancing their capabilities, improving cost savings and reliability, and diversifying the energy mix for greater efficiency compared to standalone alternatives [6].In addition, optimal integration of RE hybridization with Battery Energy Storage System (BESS) can balance the intermittence to improve reliability [7]–[9].

Reliability often conflicts with cost, making optimization essential for determining the optimal sizing of RE hybrid systems and battery energy storage systems (BESS) to achieve a suitable compromise [10]–[13]. Various studies have proposed optimization methods for hybrid energy systems, including Genetic Algorithm (GA), Particle Swarm Optimization (PSO), and Non-dominated Sorting Genetic Algorithm (NSGA-II) [14]–[16]. For instance, PSO was used in [13] to develop an optimal wind and solar PV hybrid system that minimizes the cost of electricity at high reliability, defined by Loss of Load and Loss of Power Supply Probability (LPSP). Similarly, [17] employed an enhanced PSO to minimize capital and maintenance costs for a standalone hybrid system comprising wind, solar PV, and BESS. In [12], a multi-objective PSO minimized emissions and grid electricity costs at high reliability, optimizing a grid-connected solar PV, wind, and BESS system. Likewise, [10] optimized a solar PV, wind, BESS, and diesel generator hybrid system using multi-objective PSO to minimize electricity costs while maintaining high reliability. GA was also used in [9] with MATLAB to develop an optimal hybrid system of solar PV, wind, BESS, and diesel. Another study in [18] applied GA to determine an optimal wind and solar PV configuration at minimal electricity costs while ensuring reliability. Additionally, [16] adapted a multi-objective NSGA-II to develop a mathematical model for Time-Of-Use (TOU) pricing optimization.

In [19], a multi-objective NSGA-II combined with the Python-based Pymoo framework was employed to minimize electricity costs while maximizing efficiency. This approach successfully determined an optimal grid-connected wind system with its corresponding wind turbine parameters. In a follow-up study [1], the same optimization technique was extended by incorporating a solar PV system to enhance cost efficiency and reliability through hybridization. The authors developed a model to minimize electricity costs from the grid and maximize efficiency at high reliability, resulting in an optimal grid-connected hybrid system (wind and solar PV) with ideal wind turbine parameters and solar PV module quantities. This paper extends the use of curtailed energy from renewable generation by proposing an optimal BESS dispatch strategy to reduce the redundancy of excess RE. The approach captures excess RE generation to enhance reliability and further reduce the cost of electricity purchased from the grid.

E. Mukoni and K. S. Garner are with the Department of Electrical and Electronic Engineer-ing, Stellenbosch University, Cape Town, 7600, South Africa. (email: garnerks@sun.ac.za).

To achieve this, BESS optimization is conducted using NSGA-II in conjunction with Pymoo to minimize the cost of storage and cost of electricity purchased from the electrical grid at high reliability. NSGA-II is widely recognized for its ability to efficiently explore Pareto-optimal solutions in non-convex, high-dimensional spaces, making it ideal for simultaneous optimization of cost, reliability, and efficiency in hybrid energy systems. NSGA-II provides a well-distributed Pareto front, ensuring multiple feasible solutions rather than a single local optimum, while PSO is prone to premature convergence in complex multi-objective problems, limiting exploration.

For BESS optimization, excess RE generation from the optimal grid-connected hybrid energy system and energy from the electrical grid in [1] charges the BESS and become net load demand respectively. The optimal BESS dispatch model is successfully integrated with the optimal grid-connected hybrid energy system that was obtained in [1] to supply a 2 MW PEM electrolyzer for green hydrogen production. Therefore, the proposed optimization study is successfully developed, evaluated and validated in a case study of chosen six Renewable Energy Development Zones (REDZs) in South Africa. The optimal grid-connected hybrid energy system with BESS successfully reduces the cost of electricity and curtailed energy improving the reliability. The study fills key gaps in existing research by integrating a systematic battery energy storage dispatch strategy to enhance system reliability and cost-effectiveness. The study also incorporates time-of-use tariffs into the optimization model, which is crucial for economic feasibility assessments but often overlooked in similar studies.

The grid-connected hybrid energy system components are modeled and optimized in Sections II and III respectively with the results and discussions in Section V following case study discussion in Section IV. Furthermore, the grid-connected hybrid energy system with BESS is modeled and optimized in Section VI with the results and discussions in Section VII.

II. GRID-CONNECTED HYBRID ENERGY SYSTEM MODELING

Figure 1 presents the proposed grid-connected hybrid energy system for supplying the PEM electrolyzer in green hydrogen production. In Fig. 1, wind ($P_{w,ac}$) and solar PV ($P_{s,ac}$) systems supply the PEM electrolyzer. However, due to their intermittent nature, the electrical grid ($P_{g,ac}$) system is utilized to supply insufficient energy to meet the PEM electrolyzer load demand.

The energy management system controls the supply from wind,solar PV and electrical grid systems to ensure cost savings [1]. The power from energy management system ($P_{h,ac}$) is converted to DC power ($P_{h,dc}$) which is required by the PEM electrolyzer for green hydrogen production.

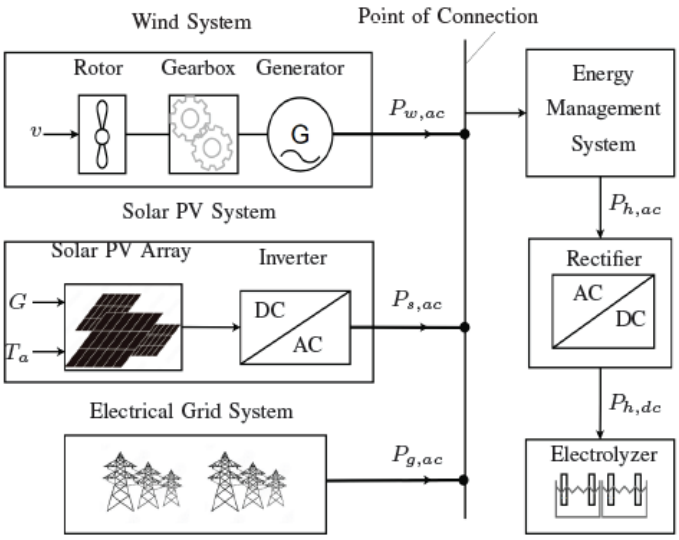

Fig. 1: Grid-connected hybrid energy system.

A. Wind System

The output power, $P_{w,ac}$ generated by the wind system varies with the wind speed at a given turbine hub-height, v calculated in [19]. Therefore, $P_{w,ac}$ is mathematically defined as [1]

$$P_{w,ac} = \begin{cases} 0 & \text{if} \quad v < v_i \text{ or } v > v_o \\ P_{w,r} & \text{if} \quad v_r \leq v \leq v_o \\ P_{q,ac} & \text{if} \quad v_i \leq v \leq v_r \end{cases}, \tag{1}$$

where v_i, v_i, v_o are cut-in, rated and cut-out wind turbine speeds. In (1), $P_{w,r}$ and $P_{q,ac}$ are calculated as [1]

$$\begin{aligned} P_{w,r} &= 0.125\pi\rho\eta_b\eta_g C_p D^2 v_r^3 \\ P_{q,ac} &= P_{w,r}(v^3 - v_i^3)/(v_r^3 - v_o^3), \end{aligned} \tag{2}$$

where η_b, η_g, C_p, ρ and D are gearbox, generator, rotor efficiencies, air density and rotor diameter respectively.

B. Solar PV System

The output power, $P_{s,ac}$ generated by the solar PV system is defined as [1]

$$P_{s,ac} = P_{s,r}\eta_{inv} G \left[1 + N_T \left(T_c - T_{stc}\right)\right] / G_{stc}, \tag{3}$$

where $P_{s,r}$, η_{inv}, G, N_T, T_c and T_a are rated DC power of the solar PV system, total number of modules in the solar PV system, DC/AC converter efficiency, solar radiance, cell and ambient temperatures respectively. G_{stc} and T_{stc} are solar radiation and temperature at standard conditions thus 1kW/m^2 and 25°C respectively [1]. In (3), T_c and $P_{s,r}$ are defined as [1]

$$\begin{aligned} T_c &= T_a + 1.25G\left(T_{noct} - 20\right), \\ P_{s,r} &= P_m N_m \end{aligned} \tag{4}$$

where T_{noct}, P_m and N_m are normal operating cell temperature, rated power of a PV module and total number of modules in the PV system respectively.

C. Electrical Grid System

The electrical grid system ($P_{g,ac}$) supplies the deficient power required to meet the PEM electrolyzer load demand, $P_{l,ac}$. $P_{g,ac}$ is defined as [1]

$$P_{g,ac} = |P_{ws,ac} - P_{l,ac}| \quad P_{g,ac} \leqslant 0 \tag{5}$$

where $P_{ws,ac}$ is defined as

$$P_{ws,ac} = P_{w,ac} + P_{s,ac}. \tag{6}$$

In (5), the excess power from wind turbine and solar PV systems is defined when ($P_{g,ac} > 0$) as

$$P_{e,ac} = |P_{ws,ac} - P_{l,ac}| \quad P_{g,ac} > 0.$$

D. Energy Management System

The energy management system in Fig. 1 ensures that $P_{g,ac}$ is supplied when necessary to allow cost savings. The energy management system power, $P_{h,ac}$ defined as [1]

$$P_{h,ac} = \begin{cases} P_{ws,ac} + P_{g,ac} & \text{if } P_{w,ac},\ P_{s,ac}, P_{ws,ac} < P_{l,ac} \\ P_{l,ac} & \text{if } P_{ws,ac},\ P_{s,ac},\ P_{w,ac} \geq P_{l,ac} \end{cases} \tag{8}$$

Using a rectifier in 1, $P_{h,ac}$ in (8) is converted to DC power to supply the PEM electrolyzer.

E. Electrolyzer

A 2 MW PEM electrolyzer, manufactured by H-TEC Systems, is utilized in this study for green hydrogen production. While detailed modeling of the electrolyzer is not performed, the specifications provided in Table I serve as guidelines for accurately sizing the grid-connected hybrid energy system to meet the required operational demands effectively.

TABLE I: Specifications of 2 MW H-TEC proton exchange membrane electrolyzer [1], [20].

Parameter	Value
Nominal power	2 MW
H_2 production	900 kg/day (420 Nm^3/hr)
Energy consumption	4.8 kWh/Nm^3 H_2
Efficiency, η_e	74%

The yearly load profile for the PEM electrolyzer is generated between 1900-2100 kW, subjected to a load factor of 0.85 with the assumption it operates throughout the year.

III. Grid-Connected Hybrid Energy System Optimization

Generally, any multi-objective optimization function consists of design variables (x), objective functions (f), constraints (g) formulated as [1]

$$\begin{aligned} \text{minimize / maximize} \quad & f_j(x) && j = 1, .., J \\ \text{subjected to.} \quad & g_k(x) \leq 0 && k = 1, .., K \\ & x_i^l \leq x_i \leq x_i^u && i = 1, .., I \\ & i, j, k \ \epsilon \ \mathbb{N} \end{aligned} \tag{9}$$

where J, K and I are the number of objective functions, constraints and design variables respectively. x_i^l and x_k^u are lower and upper boundaries of design variables.

A. Optimization Problem Formulation

Following (9), nine design variables expressed in matrix form in (10) are considered and they include wind turbine parameters and total number of solar PV modules.

$$[x] = [x_1\ x_2\ \ldots\ x_9]^T = [v_i\ v_r\ v_o\ \eta_b\ \eta_g\ C_p\ D\ H\ N_m]^T \tag{10}$$

The lower (x^l) and upper (x^u) boundaries of the design variables are subject to the designer's choice and for this study the chosen bounds are listed in Table II.

For example, the wind turbine parameters are selected based on the cut-in, cut-out and rated wind speed, while the number of PV modules are selected according to the required generation capacity. Since the optimization employs NSGA-II, an evolutionary approach, the initial population of design variables are randomly generated within the predefined boundaries using Latin Hypercube Sampling.

TABLE II: Design variables of the grid-connected hybrid energy system [1].

Parameter	Unit	Symbol	Boundaries	
		x	x_l	x_u
Cut-in speed	m/s	v_i	3.00	4.00
Rated speed	m/s	v_r	12.0	15.0
Cut-out speed	m/s	v_o	23.0	25.0
Gearbox efficiency	-	η_b	0.85	0.95
Generator efficiency	-	η_g	0.90	0.96
Rotor efficiency	-	C_p	0.40	0.50
Rotor diameter	m	D	60.0	120.0
Hub height	m	H	60.0	120.0
Number of modules	-	N_m	N_{min}	N_{max}

Using the design variables, two objective functions namely; cost of electricity purchased from the electrical grid (C_e) and efficiency (η) expressed in matrix form in (11) can be evaluated.

$$[f] = [f_1\ f_2]^T = [C_e\ \ \eta]^T. \tag{11}$$

In (11), C_e is calculated as [1]

$$C_e = (P_{g,ac}\Delta_t)\tau = E_{g,ac}\tau, \tag{12}$$

where $E_{g,ac}$ is the deficient energy from the grid with only wind and solar PV generation considered and τ is the yearly TOU tariff charge based on TOU periods.

Furthermore, η in (11) is defined as [1]

$$\eta = \eta_c \frac{P_{ws}}{P_{w,r} + P_{s,r}}, \tag{13}$$

where P_{ws} is the cumulative power from the wind turbine and solar PV systems. In (13), η_c is calculated as [1]

$$\eta_c = \eta_m \eta_r \eta_e, \tag{14}$$

where η_m, η_r, η_e are efficiencies of energy management, rectifier and electrolyzer systems in Fig 1 respectively. For this study, η_m and η_r are set to 0.90 and 0.95 respectively while η_e is given in Table I [1].

The objective functions in (11) are constrained by 2 inequality constraints expressed in matrix form as [1]

$$[g] = [g_1\ g_2]^T = [R_e\ \ P_{ws,ac}\ ]^T. \tag{15}$$

where R_e is the reliability of wind turbine and solar PV systems defined based on LPSP concept thus ratio of deficient energy supplied by the electrical grid system and PEM electrolyzer load demand. R_e is mathematically defined as [1]

$$R_e = P_{g,ac}/P_{l,ac}. \tag{16}$$

In (15), $P_{ws,ac}$ limits over-sizing the wind turbine and solar PV systems using the generated PEM electrolyzer load demand upper and lower bounds. In addition, R_e is bounded by $[0\ 1]$ thus at $R_e = 0$ and $R_e = 1$, the PEM electrolyzer load is fully and never satisfied respectively. Therefore, mathematically the (15) constraint boundaries are expressed as

$$\begin{aligned} R_{e,min} \leq R_e \leq R_{e,max}, \\ P_{l,min} \leq P_{ws,ac} \leq P_{l,max}. \end{aligned} \tag{17}$$

B. Optimization Procedure and Implementation

The grid-connected hybrid energy system is optimized following the procedure illustrated in Fig. 2 and discussed in detail as follows:

1. Evaluate $P_{w,ac}$ in (1) using initial design variables $[x]$ in (10) and determine maximum net-residual PEM electrolyzer load demand, $P_{n,max}$ using (18)

$$P_{n,max} = \max\left(|P_{l,ac} - P_{w,ac}|\right). \tag{18}$$

2. $P_{n,max}$ guides the selection of chosen solar PV module and inverter in Table III determined in [1] to calculate $P_{s,ac}$ in (3)

TABLE III: Chosen solar PV module and inverter.

Solar PV module	Sun Power SPRX22 475 COM
Inverter	Power Electronics FS2300CU15 690V

3. The deficient power from the electrical grid, $P_{g,ac}$ required to meet the PEM electrolyzer load demand when $P_{w,ac}$ and $P_{s,ac}$ are insufficient is determined using (5).
4. The initial objective functions in (11) and the constraints in (15) $[f\ g]$ are calculated using NSGA-II and passed to the interface model defined as [19]

$$u_i' = u_i + u_i^l/u_i^u - u_i^l, \tag{19}$$

where u_i' is the scaled variable between $[0\ 1]$ bounds, u_i, u_i^l, and u_i^u are the actual variable, lower and upper boundaries of u_i respectively.
5. The interface model in Fig. 2, scales $[x]$ to $[x']$ in order to give equal dominance and ensure satisfactory global solution from NSGA-II. As a result, the scaled objective functions and constraints are $[f'\ g']$.
6. NSGA-II repeats the steps above using new generated $[x]$ values until convergence is achieved based on the chosen NSGA-II operators. A Pareto front is formulated upon convergence and a single optimal solution of $[x\ f\ g]$ is determined using multi-criteria decision making.

To implement the optimization procedure in Fig. 2, a python framework, Pymoo which offers multi-objective NSGA-II and multi-criteria decision making techniques to find the optimal solution from a Pareto front upon convergence [1].

In Pymoo, only pure minimization of objectives is possible, therefore, to maximize any objective a multiple of -1 is used to define it for minimization [21]. As a result, (11) becomes [1]

$$\begin{bmatrix} f_1 \\ f_2 \end{bmatrix} = \begin{bmatrix} E_{g,ac}\tau \\ -\eta_c(P_{ws}/(P_{w,r} + P_{s,r})) \end{bmatrix}. \tag{20}$$

Additionally, in Pymoo, the formulation of constraints must be less than or equal to zero ($\leqslant 0$). Therefore, the constraints in (15) become [1]

$$\begin{bmatrix} g_1 \\ g_2 \end{bmatrix} = \begin{bmatrix} -P_{ws,ac} + P_{l,min}\ , P_{ws,ac} - P_{l,max} \\ -R_e + R_{e,min}\ , (R_e - R_{e,max}) \end{bmatrix}\ g_1,\ g_2\ \leqslant 0. \tag{21}$$

Furthermore, the optimal solution in Fig. 2 is determined using multi-criteria decision making technique in Pymoo [21].

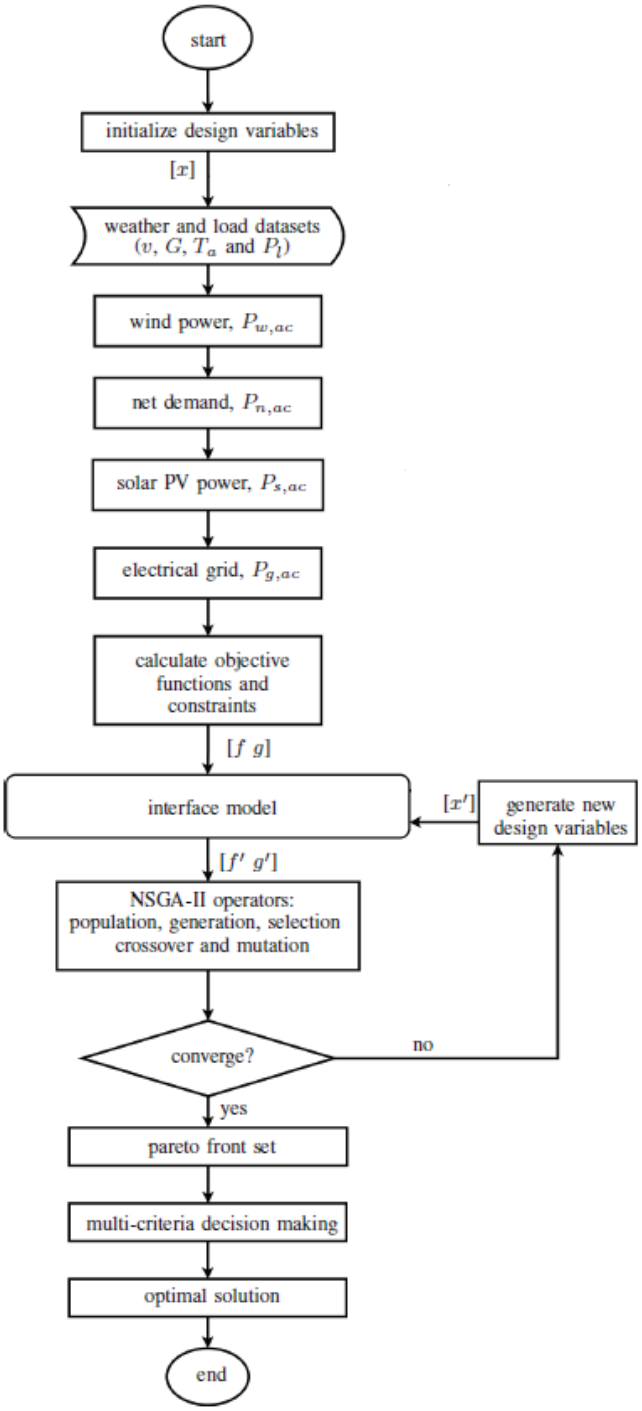

Fig. 2: Grid-connected hybrid energy system optimization procedure.

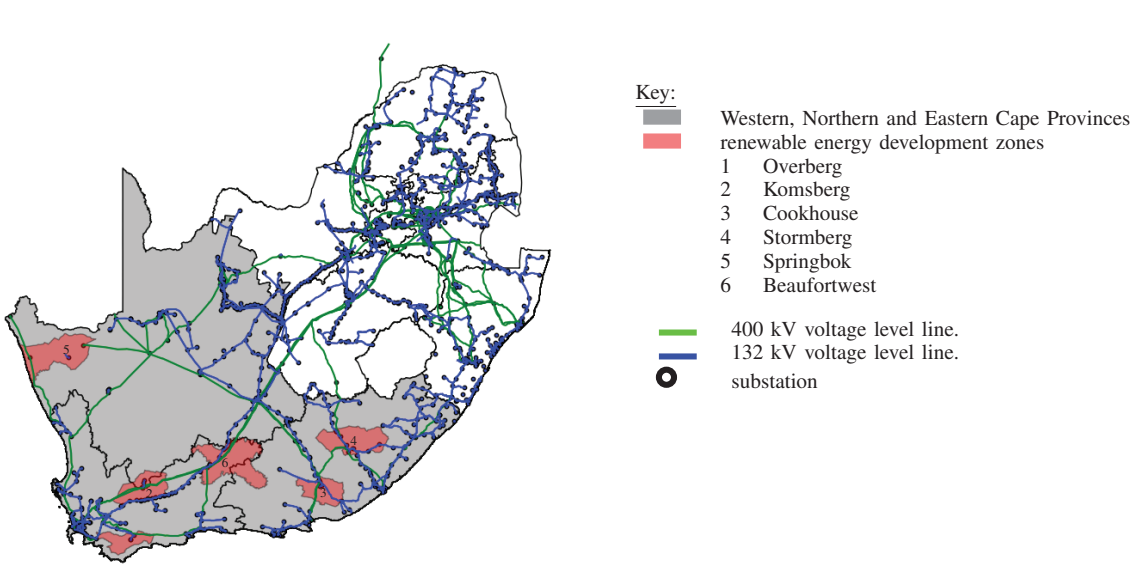

Fig. 3: The chosen six REDZs [24].

IV. Case Study: Site Description and Data

The case study is based on six REDZs in South Africa shown in Fig. 3, chosen because of they have both high wind and solar resources for large-scale RE development [19]. The REDZs are a study conducted to support large-scale RE development in South Africa through with limited environmental impacts [22], [23].

In addition, the REDZs in Fig. 3 have electrical grid infrastructure, both substation and overhead lines for transmission, voltage support and supply of energy when the RE resources are insufficient. The wind data for REDZs in Fig. 3 were obtained from Wind Atlas South Africa as 10-minute interval wind speed data at 60m anemometer height [25]. The average wind speed and respective standard deviation for each of the REDZs are listed in Table IV [19].

TABLE IV: Annual average wind speed and standard deviation of the six REDZs [24].

REDZs	Mean speed (m/s)	Standard deviation (m/s)
Overberg	8.04	4.00
Komsberg	7.15	3.34
Cookhouse	6.97	3.57
Stormberg	6.46	3.23
Springbok	7.21	2.90
Beaufortwest	6.65	3.00

The REDZs all have relatively high wind speeds, with highest and lowest wind speeds in Overberg and Stormberg respectively. Furthermore, Table IV gives standard deviation to show consistency of the wind speed. Where, low and high standard deviation in (Springbok and Beaufortwest) and Overberg thus wind consistency and inconsistency respectively.

For solar data, the solar radiance, G and ambient temperature, T_a listed in Table V are obtained through processing Typical Meteorological Year data using System Advisor Model [26].

TABLE V: Annual average solar radiance and ambient temperatures of the six REDZs [24].

REDZs	Solar radiance (kW/m^2)	Temperature (°C)
Overberg	0.191	17.1
Komsberg	0.212	17.1
Cookhouse	0.226	17.8
Stormberg	0.237	15.6
Springbok	0.250	17.6
Beaufortwest	0.243	18.3

The REDZs have relatively high solar resources with the highest and lowest solar radiance are in Springbok and Overberg respectively.

V. Grid-Connected Hybrid Energy System: Results and Discussions

Since the case study is based in South Africa, following discussion in Section IV, the electrical grid system discussed in II-C represents Eskom, the respective grid system operator [27]. For this study, the deficient energy from the electrical grid is assumed to be from Eskom's wind farm of 100 MW [28] Therefore, the cost of electricity purchased from the electrical grid in (12) relies on the published TOU periods and charges in Fig. 4 and Table VI respectively.

Low demand season: September to May

Hours	1	2	3	4	5	6	7	8	9	10	11	12	13	14	15	16	17	18	19	20	21	22	23	24
Weekdays	O	O	O	O	O	O	S	P	P	P	S	S	S	S	S	S	S	S	P	P	S	S	O	O
Saturday	O	O	O	O	O	O	O	S	S	S	S	S	O	O	O	O	O	O	S	S	O	O	O	O
Sunday	O	O	O	O	O	O	O	O	O	O	O	O	O	O	O	O	O	O	O	O	O	O	O	O

High demand season: June to August

Hours	1	2	3	4	5	6	7	8	9	10	11	12	13	14	15	16	17	18	19	20	21	22	23	24
Weekdays	O	O	O	O	O	O	P	P	P	S	S	S	S	S	S	S	S	P	P	S	S	S	O	O
Saturday	O	O	O	O	O	O	S	S	S	S	S	O	O	O	O	O	O	O	S	S	O	O	O	O
Sunday	O	O	O	O	O	O	O	O	O	O	O	O	O	O	O	O	O	O	O	O	O	O	O	O

Fig. 4: Low and high demand seasons TOU periods [27].

In Fig. 4, the TOU periods: peak (P), standard (S) and offpeak (O) are defined f or e ach d emand s eason: (high demand: June to August) and (low demand: September to May). The TOU charges in Table VI are in South African Rand (R) excluding VAT. In addition, they are determined based on the transmission zones thus location of the load [19], [27]. Therefore, in this study, the load or PEM electrolyzer is assumed to be located in the REDZs.

Following the optimization procedure in Fig. 2, using operators given in Table VII, NSGA-II in conjunction with Pymoo is utilized to solve the objective, constraints and design variables of the grid-connected hybrid energy system.

TABLE VI: Eskom TOU tariff charges for 2022/2023 [27].

Energy Charges (R/kWh)			
Cookhouse, Stormberg and Beaufortwest			
	Peak	Standard	Off Peak
Low demand	1.4984	1.0314	0.6543
High demand	4.5935	1.3917	0.7557
Overberg, Komsberg and Springbok			
	Peak	Standard	Off Peak
Low demand	1.5131	1.0412	0.6607
High demand	4.6392	1.4052	0.7628

TABLE VII: Chosen NSGA-II operating parameters [1].

Operator	Parameter
Population Size	200
Number of off-springs	200
Number of generations	300
Sampling	Random
Crossover (Probability of crossover)	Simulated Binary (0.9)
Mutation	Polynomial

In Table VII, the number of generations determine convergence upon which a Pareto front is formulated. As a result, the scaled objective functions, $[C'_e \ \ \eta']$ shown in Fig. 2 are obtained and presented in Fig. 5 for each REDZ together with the respective Optimal Solution (OS).

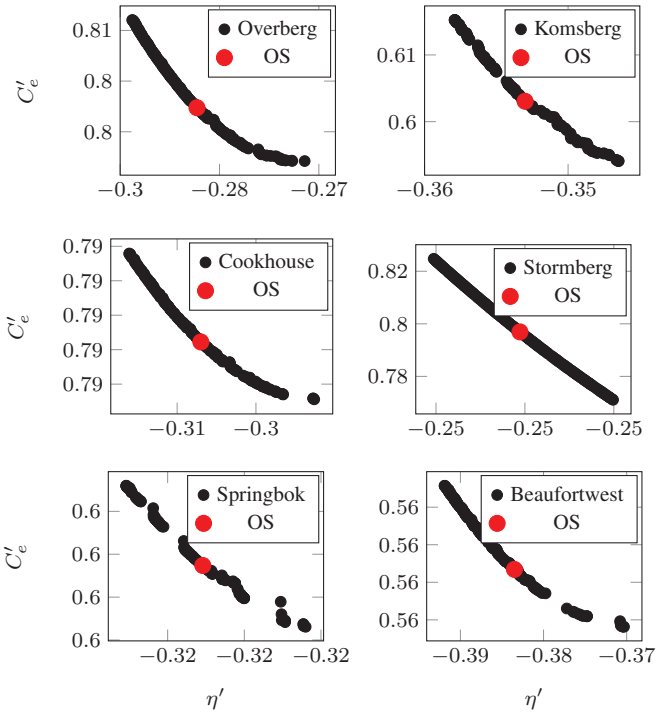

Fig. 5: Scaled Pareto fronts of the grid-connected hybrid energy system for the six REDZs [1].

From the Pareto front in Fig. 5, OS is identified using the multi-criteria decision making method namely; compromise programming available in Pymoo [21]. Following Fig. 2, the actual optimal solutions of objective functions, $[C_e \ \eta]$ in (11) and constraints, $[R_e \ P_{ws,ac}]$ in (15) are listed in Table VIII for each REDZ.

TABLE VIII: Actual optimal objectives and constraints of the grid-connected hybrid energy system for the six REDZs [1]

REDZs	C_e (R' million)	η	R_e	$P_{ws,ac}(kW)$
Overberg	7.97	0.29	0.35	2 470
Komsberg	6.05	0.36	0.27	2 471
Cookhouse	7.88	0.30	0.35	2 470
Stormberg	7.97	0.25	0.37	2 342
Springbok	5.95	0.32	0.26	2 471
Beaufortwest	5.59	0.38	0.22	2 471

From Table VIII, because of Beaufortwest's wind and solar consistency, it resulted in low cost of electricity purchased from the electrical grid, high efficiency and reliability. This is true for REDZs with inconsistent wind in Overberg which gives high cost of electricity, low efficiency and reliability even though the average wind speed is high.

The actual optimal design variables in (10) that calculated the optimal objective functions and constraints in Table VIII are listed in Table IX.

TABLE IX: Actual optimal design variables of the grid-connected hybrid energy system for the six REDZs [1].

REDZs	v_i	v_r	v_o	η_b	η_g	C_p	D	H	N_m
Overberg	3	12	23	0.95	0.96	0.45	118	60	7026
Komsberg	3	12	25	0.95	0.96	0.45	102	119	6284
Cookhouse	3	12	25	0.95	0.96	0.46	120	114	6663
Stormberg	3	12	25	0.95	0.96	0.50	120	120	7018
Springbok	3	12	25	0.95	0.96	0.50	108	120	6074
Beaufortwest	3	12	25	0.95	0.96	0.43	97.0	120	6526

With the optimal design variables known, the average powers of $\{(P_{w,r}, P_{w,ac}), (P_{s,r}, P_{s,ac}), P_{g,ac}$ and $P_{e,ac}\}$ calculated in (1), (3), (5) and (7) respectively are given in Table X. In addition, the annual average PEM electrolyzer load demand $(P_{l,ac})$ obtained following discussion in Section II-E is given in Table X.

TABLE X: Optimal average annual powers in kW of the grid-connected hybrid energy system for the six REDZs.

REDZs	$P_{w,r}$	$P_{w,ac}$	$P_{s,r}$	$P_{s,ac}$	$P_{l,ac}$	$P_{g,ac}$	$P_{e,ac}$
Overberg	5 267	1 846	3 347	624	2 354	831	948
Komsberg	3 938	1 849	2 994	622	2 354	635	752
Cookhouse	4 965	1 769	3 175	701	2 354	826	943
Stormberg	5 985	1 565	3 344	777	2 354	863	852
Springbok	4 772	1 763	2 894	708	2 354	610	727
Beaufortwest	3 332	1 732	3 110	739	2 354	511	628

VI. Grid-Connected Hybrid Energy System With Battery Energy Storage System

Following Sections IV and V respectively, it is evident that the challenge with RE (wind and solar), is that resources availability does not always coincide with the load demand. This is problematic especially for a hybrid energy system connected to an electrical grid which do not allow supply of excess energy back to the grid, thus, energy is lost. To quantify

the lost energy, a new term, curtailment ratio, is introduced following (6) and (7), expressed as

$$R_c = \sum_t P_{e,ac} / \sum_t P_{ws,ac}. \tag{22}$$

Thus, from (22), curtailment ratio is defined as the RE total annual excess energy to the corresponding production of RE energy. Table XI gives the curtailment ratios and it is evident that a lot of RE energy (up to approximately 38%) is lost.

TABLE XI: Curtailment ratios of the grid-connected hybrid energy system for the six REDZs.

REDZs	R_c (%)
Overberg	38.4
Komsberg	30.4
Cookhouse	38.2
Stormberg	36.4
Springbok	29.4
Beaufort West	25.4

To mitigate the problem of losing such amount of energy, the paper extend the studies by utilizing BESS. Rechargeable BESS allow RE systems to store the excess energy for later use. This process is called energy shifting, which enables RE generation coincide with the load [29]–[32].

The following sections illustrates the approach adopted to optimally size the BESS by utilizing the excess energy in return, further minimizing and maximizing the system cost of electrical grid and reliability respectively. The same optimization algorithm used in Section III is also utilized in finding the optimal BESS size.

A. Battery Energy Storage System Optimization

Following (9), the BESS optimization considers two design variables with direct impact on the performance of the BESS and are expressed in matrix form as

$$[x_9 \ x_{10}]^T = [P_{b,r} \ D_b]^T, \tag{23}$$

where $P_{b,r}$ and D_b are the BESS rated power and duration respectively, with their chosen lower and upper boundaries given in Table XII.

TABLE XII: Design variables for the battery energy storage system.

Parameter	Unit	Symbol	Boundaries	
		x_i	x^l	x^u
BESS rated power	kWh	$P_{b,r}$	1 000	20 000
BESS duration	hour	D_b	1	8

By varying the design variables of (23) using values given in Table XII, an optimal BESS size is obtained by minimizing two objectives functions expressed in matrix form as

$$[f_3 \ f_4]^T = [C_s \ \ C_{e_n}]^T. \tag{24}$$

In (24), C_s is the cost of storage calculated as

$$C_s = C_{cap} C_b / \sum_t P_{d,ac}. \tag{25}$$

where C_{cap} is the BESS fixed CAPEX which is taken as R4 000/kWh [33]–[35] and $P_{d,ac}$ is the BESS dispatch power. In (25), C_b is the BESS rated capacity and it is calculated as

$$C_b = P_{b,r} D_b \tag{26}$$

Furthermore, in (24), C_{e_n} is the cost of electricity purchased from the grid after BESS integration and is calculated as

$$C_{e_n} = (P_{g_n,ac} \Delta_t)\tau = E_{g_n,ac}\tau, \tag{27}$$

τ is calculated as discussed in Section III-A and $P_{g_n,ac}$ is the power supplied by the electrical grid after the BESS is considered with the wind and solar PV systems defined as

$$P_{g_n,ac} = |(P_{ws,ac} + P_{d,ac}) - P_{l_n,ac}| \quad P_{g_n,ac} \leqslant 0 \tag{28}$$

where $P_{l_n,ac}$ is equivalent to the power supplied by the electrical grid when BESS was not considered in (5).

It is important to note that, minimizing (25), maximizes $P_{d,ac}$, thereby reducing the lost energy which in turn increases the system reliability. For a feasible design, the objective functions of (24), are constrained by the system reliability given by

$$[g_3] = [R_{e_n}], \tag{29}$$

where R_{e_n} is the reliability of wind, solar PV and BESS generation systems defined as

$$R_{e_n} = P_{g_n,ac} / P_{l_n,ac}. \tag{30}$$

Thus, constraints in (29) become

$$R_{e_n,min} \leq R_{e_n} \leq R_{e_n,max}. \tag{31}$$

In (31), R_{e_n} is bounded by [0 1] thus at $R_{e_n,min} = 0$ and $R_{e_n,max} = 1$ the PEM electrolyzer load is fully and never satisfied respectively.

B. Battery Energy Storage System Dispatch Management System

The BESS is dispatched in such a way that if the wind and solar PV excess power ($P_{e,ac}$) is greater than the electrolyzer net-load ($P_{l_n,ac}$), the BESS will charge until full and the reverse process is true. The BESS round-trip efficiency (n_b) is taken as losses when the BESS is discharging and it is taken as 85% [36]–[38].

Thus, at a point given in time (t), the actual battery discharge $P_{d,ac}$ and charge $P_{c,ac}$ is calculated by comparing the RE excess power $P_{e,ac}$ with the net-load $P_{l_n,ac}$ as

$$\begin{aligned} P_{d,ac} &= \min(P_{md}, \max(0, P_{l_n,ac})), \\ P_{c,ac} &= \min(P_{mc}, \max(0, P_{e,ac})), \end{aligned} \tag{32}$$

where P_{md} and P_{mc} are the BESS maximum discharge and charge power respectively, given by [39]

$$\begin{aligned} P_{md} &= \min(P_{b,r}, S_{b(t-1)}\eta_b) \\ P_{mc} &= \min(P_{b,r}, C_b - S_{b(t-1)}). \end{aligned} \tag{33}$$

In (33), $P_{b,r}$ and C_b are given in (25) and the state of charge S_b is given as [40]

$$S_b = S_{b(t-1)} + P_{c,ac} - P_{d,ac}/\eta_b. \tag{34}$$

VII. Grid-Connected Hybrid Energy System With Battery Energy Storage System: Results and Discussions

Following the grid-connected hybrid energy system with BESS discussed in Sections VI, the NSGA-II optimization algorithm is used to search for the optimal BESS size using the BESS dispatch management system discussed in Section VI-B. The NSGA-II operators as given in Table VII are utilized to achieve convergence upon which the Pareto fronts in Fig. 6 for all the REDZs is formulated. In addition, the OS determined using multi-criteria decision making in Pymoo is presented for each REDZs in Fig. 6.

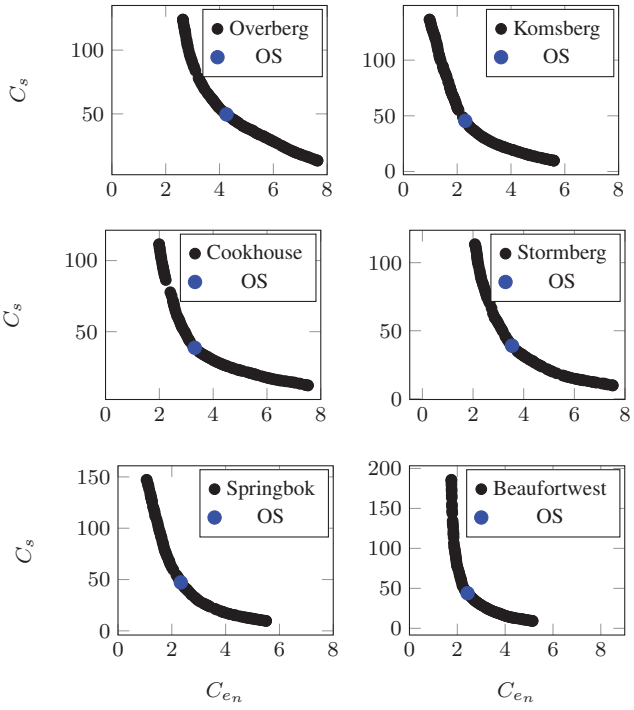

Fig. 6: Pareto fronts of the battery energy storage system for the six REDZs.

Using compromise programming discussed in Section V, the optimal solutions for the objective and constraints for each REDZs shown in Fig. 6 are listed in Table XIII.

TABLE XIII: Optimal objective functions and constraints for the battery energy storage system for the six REDZs.

REDZs	C_s (R/kWh)	C_{e_n} (R' million)	R_{e_n}
Overberg	49.6	4.26	0.183
Komsberg	45.5	2.30	0.092
Cookhouse	38.7	3.32	0.133
Stormberg	37.9	3.54	0.150
Springbok	47.2	2.34	0.096
Beaufortwest	43.9	2.43	0.074

The optimal solution of design variables,$[P_{b,r}\ D_b]$ in (23) as well as the BESS capacity, C_b in (26) for the BESS optimization are given in Table XIV for each REDZs. Using the optimal design variables of Table XIV, the calculated curtailment ratio in (22) of the grid-connected hybrid energy system with battery energy storage system considered for each REDZs are given in Table XV.

TABLE XIV: Optimal design variables for the battery energy storage system for the six REDZs.

REDZs	$P_{b,r}$ (kW)	D_b (hours)	C_b (kWh)
Overberg	6220	7	43 540
Komsberg	5940	7	41 580
Cookhouse	5430	8	43 440
Stormberg	7180	6	43 080
Springbok	13190	3	39 570
Beaufortwest	8110	4	32 440

TABLE XV: Curtailment ratios of the grid-connected hybrid energy system with battery energy storage system for the six REDZs.

REDZs	R_{c_n} (%)
Overberg	20.3
Komsberg	11.6
Cookhouse	15.0
Stormberg	12.4
Springbok	12.2
Beaufortwest	10.2

It is evident that with the consideration of BESS, the curtailment ratios of the grid-connected hybrid energy system in Table XI have improved as given in Table XV thus the lost or curtailed energy has been reduced.

To have a comprehensive analysis the cost of electricity, reliability and curtailment ratio of both systems (i.e., without and with BESS), the percentage improvements between the two systems are tabulated in Table XVI.

TABLE XVI: Percentage improvement of cost of electricity, reliability and curtailment ratio for the six REDZs.

REDZs	Cost of electricity (%)	Reliability (%)	Curtailment ratio (%)
Overberg	46.6	48.2	47.1
Komsberg	62.0	65.8	62.0
Cookhouse	58.0	62.0	60.6
Stormberg	55.6	58.7	66.0
Springbok	60.8	63.0	58.5
Beaufortwest	56.6	66.4	59.7

From Table XVI, there is an improvement of $46 - 66\%$ in the cost of electricity, reliability and curtailment ratio. Thus, adoption of optimal BESS size in RE generation system does not only improve the curtailment ratio or lost energy of RE generation system but also reduce further the cost of electricity purchased from the electrical grid therefore, increasing reliability.

VIII. Conclusion

The grid-connected hybrid energy system was successfully developed and mathematically formulated to optimize cost of electricity, efficiency, and reliability while incorporating renewable energy generation constraints. The optimization approach, implemented using NSGA-II in conjunction with Pymoo, effectively identified Pareto-optimal solutions that minimize electricity costs and curtailment while maximizing system reliability.

The results demonstrate that the optimization process avoids local minima, ensuring robust and practical outcomes. A key contribution of this study is the integration of a battery energy storage system (BESS), which significantly enhances the feasibility of renewable energy adoption by curtailment losses (by up to 66%) and improving system reliability (by 40–66%). The optimized BESS dispatch strategy ensures that excess renewable energy is efficiently stored and and utilized, reducing dependence on grid electricity.

These findings provide valuable insights for policymakers and energy planners in South Africa. The demonstrated cost reductions and reliability improvements support scalability and feasibility assessments for future grid-connected hybrid renewable systems. Specifically:

i. The study highlights the need for policy incentives that encourage the deployment of energy storage systems to complement variable renewable energy sources.

ii. The results underscore the importance of time-of-use (TOU) tariffs in optimizing grid-connected hybrid systems, suggesting that revised tariff structures could enhance economic viability.

iii. The optimization approach can be adopted in national energy planning models to improve renewable energy penetration in the South African grid while ensuring system stability and affordability.

iv. The case study of six Renewable Energy Development Zones (REDZs) provides a replicable framework for identifying optimal sites for future large-scale renewable energy projects.

In conclusion, this study demonstrates that optimal integration of energy storage with renewables can significantly enhance South Africa's energy transition by reducing reliance on fossil fuels, lowering electricity costs, and increasing energy security. Future work can focus on extending this approach to larger-scale energy systems, incorporating hydrogen storage, and refining grid flexibility strategies to further support South Africa's decarbonization goals.

ACKNOWLEDGMENT

The authors acknowledge the support of the National Research Foundation of South Africa under grant number 138307.

REFERENCES

[1] E. Mukoni, K. S. Garner, and C. Van Staden, "Hybrid system optimization model for hydrogen production, case study: South Africa," in *2023 IEEE International Conference on Environment and Electrical Engineering and 2023 IEEE Industrial and Commercial Power Systems Europe (EEEIC /ICPS Europe)*, 2023, pp. 1–6.

[2] United Nations, "The Paris Agreement," Available Online: https://www.un.org/en/climatechange/paris-agreement, 2015, (accessed 20 January 2022).

[3] "Optimal energy management and control aspects of distributed microgrid using multi-agent systems," *Sustainable Cities and Society*, vol. 44, pp. 855–870, 2019. [Online]. Available: https://www.sciencedirect.com/science/article/pii/S2210670718315233

[4] "The Future of Hydrogen – Analysis," [Available Online]: https://www.iea.org/reports/the-future-of-hydrogen, 2019, (accessed 25 February 2022).

[5] "International energy agency (iea): Global Hydrogen Review – Analysis," Available Online: https://www.iea.org/reports/global-hydrogen-review-2021, 2021, (accessed 25 February 2022).

[6] P. Dalwadi, V. Shrinet, C. R. Mehta, and P. Shah, "Optimization of solar-wind hybrid system for distributed generation," in *2011 Nirma University International Conference on Engineering*, 2011, pp. 1–4.

[7] T.-T. Nguyen and T. Boström, "Multiobjective optimization of a hybrid wind/solar battery energy system in the arctic," *Journal of Renewable Energy*, vol. 2021, 04 2021.

[8] G. Gursoy and M. Baysal, "Improved optimal sizing of hybrid pv/wind/battery energy systems," in *2014 International Conference on Renewable Energy Research and Application (ICRERA)*, 2014, pp. 713–716.

[9] N. Yimen, T. Tchotang, A. Kanmogne, I. Abdelkhalikh Idriss, B. Musa, A. Aliyu, E. C. Okonkwo, S. I. Abba, D. Tata, L. Meva'a, O. Hamandjoda, and M. Dagbasi, "Optimal sizing and techno-economic analysis of hybrid renewable energy systems—a case study of a photovoltaic/wind/battery/diesel system in fanisau, northern nigeria," *Processes*, vol. 8, no. 11, 2020. [Online]. Available: https://www.mdpi.com/2227-9717/8/11/1381

[10] A. Parizad and K. J. Hatziadoniu, "Multi-objective optimization of pv/wind/ess hybrid microgrid system considering reliability and cost indices," in *2019 North American Power Symposium (NAPS)*, 2019, pp. 1–6.

[11] Z. Medghalchi and O. Taylan, "A novel hybrid optimization framework for sizing renewable energy systems integrated with energy storage systems with solar photovoltaics, wind, battery and electrolyzer-fuel cell," *Energy Conversion and Management*, vol. 294, p. 117594, 10 2023.

[12] L. Wang and C. Singh, "Pso-based multi-criteria optimum design of a grid-connected hybrid power system with multiple renewable sources of energy," in *2007 IEEE Swarm Intelligence Symposium*, 2007, pp. 250–257.

[13] A. Nekkache, B. Bouzidi, A. Kaabeche, and Y. Bakelli, "Hybrid pv-wind based water pumping system optimum sizing: a pso-llp-lpsp optimization and cost analysis," in *2018 International Conference on Electrical Sciences and Technologies in Maghreb (CISTEM)*, 2018, pp. 1–6.

[14] S. K. Ramoji, "Optimum design of a hybrid pv/wind energy system using genetic algorithm (ga)," *IOSR Journal of Engineering*, vol. 4, pp. 38–48, 01 2014.

[15] W. Zhang, X. Li, M. Cheng, and J. Wang, "A comparative study of ga, pso, and nsga-ii for solving the economic dispatch problem in power systems," *IEEE Transactions on Power Systems*, 2013.

[16] Jiang, Liu, Wang, and Zheng, "Multiobjective tou pricing optimization based on nsga2," vol. 2014, 2014.

[17] G. M. Karve, K. M. Kurundkar, and G. A. Vaidya, "Implementation of analytical method and improved particle swarm optimization method for optimal sizing of a standalone pv/wind and battery energy storage hybrid system," in *2019 IEEE 5th International Conference for Convergence in Technology (I2CT)*, 2019, pp. 1–5.

[18] X. Chang, Z. Qi, and J. Guo, "Optimal configuration of wind solar hybrid power generation system," in *2015 IEEE International Conference on Progress in Informatics and Computing (PIC)*, 2015, pp. 566–569.

[19] E. Mukoni and K. S. Garner, "Multi-objective non-dominated sorting genetic algorithm optimization for optimal hybrid (wind and grid)-hydrogen energy system modelling," *Energies*, vol. 15, no. 19, p. 7079, 2022.

[20] "H-TEC PEM Electrolysers HCS: H-TEC SYSTEMS products," Available Online: https://www.h-tec.com/en/products/detail/h-tec-pem-elektrolyseur-hcs/10-mw-hcs/, (accessed on 28 April 2022).

[21] J. Blank and K. Deb, "Pymoo: Multi-Objective Optimization in Python," *IEEE Access*, vol. 8, pp. 89 497–89 509, 2020. [Online]. Available: https://ieeexplore.ieee.org/document/9078759/

[22] "Department of environment affairs (dea) and council of scientific and industrial research (csir): Strategic environmental assessment for wind

and solar photovoltaic energy in south africa," Stellenbosch, Western Cape, 2015. [Online]. Available: https://egis.environment.gov.za/redz
[23] "Department of environment affairs (dea) and council of scientific and industrial research (csir): Phase 2 strategic environmental assessement for wind and solar pv energy in south africa," Stellenbosch, Western Cape, 2019. [Online]. Available: https://egis.environment.gov.za/redz
[24] E. Mukoni, "Masters thesis: Grid-connected hybrid energy system modeling and optimization study for green hydrogen production in south africa," Stellenbosch University, pp. 1–85, December, 2023. [Online]. Available: https://scholar.sun.ac.za/server/api/core/bitstreams/2f1da4e2-739d-4ac2-9a7c-04cf75bbb230/content
[25] "Wind Atlas for South Africa (WASA) SANEDI," Available Online: https://wasaproject.info/, 2022, (accessed on 22 March 2022).
[26] "System Advisor Model - SAM," https://sam.nrel.gov/, 2023, accessed: March 1, 2023.
[27] "Eskom tariffs and charges (2022/2023) - Distribution," Available Online: https://www.eskom.co.za/distribution/tariffs-and-charges/, 2022, (accessed on 28 April 2022).
[28] Eskom, "Integrated report 31 march 2021," 2021, [Online].Available: https://www.eskom.co.za/wp-content/uploads/2021/08/2021IntegratedReport.pdf.
[29] R. Barzin, J. J. Chen, B. R. Young, and M. M. Farid, "Peak load shifting with energy storage and price-based control system," *Energy*, vol. 92, pp. 505–514, 2015, sustainable Development of Energy, Water and Environment Systems. [Online]. Available: https://www.sciencedirect.com/science/article/pii/S0360544215007689
[30] Y. Zhang, P. Kou, Z. Zhang, R. Tian, Y. Yan, and D. Liang, "Optimal sizing and siting of bess in high wind penetrated power systems: A strategy considering frequency and voltage control," *IEEE Transactions on Sustainable Energy*, vol. 15, no. 1, pp. 642–657, 2024.
[31] R. A. Campos, M. Braga, L. Nascimento, R. Rüther, and G. Simões, "The role of second life li-ion batteries in avoiding generation curtailment in utility-scale wind + solar parks in brazil," in *2019 IEEE 46th Photovoltaic Specialists Conference (PVSC)*, 2019, pp. 2078–2081.
[32] D. Kim, H. Kim, and D. Won, "Operation strategy of shared ess based on power sensitivity analysis to minimize pv curtailment and maximize profit," *IEEE Access*, vol. 8, pp. 197 097–197 110, 2020.
[33] E. Vartiainen, G. Masson, D. Moser, and E. Roman, "Impact of weighted average cost of capital, capital expenditure, and other parameters on future utility-scale pv levelised cost of electricity," *Progress in Photovoltaics: Research and Applications*, vol. 28, 08 2019.
[34] D. Feldman, V. Ramasamy, R. Fu, A. Ramdas, J. Desai, and R. Margolis, "U.s. solar photovoltaic system and energy storage cost benchmark: Q1 2020," National Renewable Energy Lab. (NREL), Golden, CO (United States), Tech. Rep., January 27 2021. [Online]. Available: https://doi.org/10.2172/1764908
[35] W. Cole, A. W. Frazier, and C. Augustine, "Cost projections for utility-scale battery storage: 2021 update," National Renewable Energy Laboratory, Golden, CO, Technical Report, 2021. [Online]. Available: https://www.nrel.gov/docs/fy21osti/79236.pdf
[36] B. Battke, T. S. Schmidt, D. Grosspietsch, and V. H. Hoffmann, "A review and probabilistic model of lifecycle costs of stationary batteries in multiple applications," *Renewable and Sustainable Energy Reviews*, vol. 25, pp. 240–250, 2013. [Online]. Available: https://www.sciencedirect.com/science/article/pii/S136403211300275X
[37] M. Koller, T. Borsche, A. Ulbig, and G. Andersson, "Review of grid applications with the zurich 1mw battery energy storage system," *Electric Power Systems Research*, vol. 120, pp. 128–135, 2015, smart Grids: World's Actual Implementations. [Online]. Available: https://www.sciencedirect.com/science/article/pii/S0378779614002326
[38] K. Mongird, V. Viswanathan, J. Alam, C. Vartanian, V. Sprenkle, and R. Baxter, "2020 grid energy storage technology cost and performance assessment," USDOE, Tech. Rep., December 2020. [Online]. Available: https://www.energy.gov/energy-storage-grand-challenge/downloads/2020-grid-energy-storage-technology-cost-and-performance
[39] A. Ibáñez-Rioja, L. Järvinen, P. Puranen, A. Kosonen, V. Ruuskanen, K. Hynynen, J. Ahola, and P. Kauranen, "Off-grid solar pv–wind power–battery–water electrolyzer plant: Simultaneous optimization of component capacities and system control," *Applied Energy*, vol. 345, p. 121277, 2023. [Online]. Available: https://www.sciencedirect.com/science/article/pii/S0306261923006414
[40] Y. Yang, C. Menictas, S. Bremner, and M. Kay, "A comparison study of dispatching various battery technologies in a hybrid pv and wind power plant," 2018, pp. 1–5.

Esmeralda Mukoni, was born in Zimbabwe on January 24, 1995. She completed the B. Eng degree in Electrical and Electronic Engineering at Stellenbosch University in 2020 and the M. Eng degree (Cum Laude) in Electrical Engineering at Stellenbpsch University in 2022.

Her expertise spans renewable energy modeling, optimization algorithms, and the practical application of hybrid systems for green hydrogen production. Her contributions support South Africa's transition toward a sustainable energy future.

Karen S. Garner (M'17-SM'2024) was born in Cape Town, South Africa on October 17, 1985. She completed the B. Eng degree in Electrical and Electronic Engineering at Stellenbosch University in 2007, the M. Eng degree in Electrical Engineering at North-West University in 2015 and the Ph.D. degree in Electrical Engineering from Stellenbosch University in December 2021. She worked as an electrical engineer in the petrochemical industry from 2008 to 2016, completing multi-billion dollar projects from concept to construction. She is now working as a lecturer at Stellenbosch University. She is registered as a Professional Engineer in South Africa, a senior member of IEEE and SAIEE, and is supported by the South African National Research Foundation. She has received the best paper in Rotating Machines at the Southern African Power Universities Conference in 2023 and 2024. She is also a recipient of the 2024 TWAS-DFG Cooperation Visit grant. Her research interests are novel electric machines, renewable energy and power transmission.

CONTENTS PAGE